**International Journal of Systems Science and Applied Mathematics**
2026; 11(3): 62-77
10.11648/j.ijssam
doi: 10.11648/j.ijssam.20261103.12

# Climate-Driven Differential Dynamics of Vector-Borne Diseases in the Niger-Delta: Mathematical Modelling and Environmental Health Policy Implications

**Suit Patrick Oghenerhoro[1], Henry Etaroghene Egbogho[2, *]**

[1]Department of Environmental Management and Toxicology, Dennis Osadebay University, Asaba, Nigeria
[2]Department of Mathematics, Dennis Osadebay University, Asaba, Nigeria

## Email address:

suit.oghenerhoro@dou.edu.ng (Suit Patrick Oghenerhoro), egbogho.henry@dou.edu.ng (Henry Etaroghene Egbogho)

## To cite this article:

Suit Patrick Oghenerhoro, Henry Etaroghene Egbogho. (2026). Climate-Driven Differential Dynamics of Vector-Borne Diseases in the Niger-Delta: Mathematical Modelling and Environmental Health Policy Implications. *International Journal of Systems Science and Applied Mathematics, 11*(3), 62-77. https://doi.org/10.11648/j.ijssam.20261103.12

**Received:** 13 June 2026; **Accepted:** 13 June 2026 **Published:** 23 September 2026

**Abstract:** Climate change has become one of the biggest environmental problems shaping public health worldwide, mainly when viewing its impact on vector-borne diseases. In the Niger-Delta area of Nigeria, there are ecological conditions that promote the increase of disease vectors, like mosquitoes, sandflies, and ticks, and this is a significant concern. Higher temperatures, shifting rainfall trends, repeated flooding episodes, and humidity swings have altered vector ecology and increased the danger of disease spread. In this work, a climate-sensitive host vector mathematical model is developed to explore how vector-borne diseases change over time under evolving environmental conditions in the Niger-Delta region. The model is developed based on a system of nonlinear differential equations that tracks the interactions between people in susceptible, exposed, infectious, and recovered groups, along with climate- dependent vector populations. In this setting, several core mathematical properties are confirmed, like positivity and boundedness, plus the existence and uniqueness of solutions. Then the disease-free equilibrium, as well as the endemic equilibrium, are derived and analyzed. With the next-generation matrix method, the basic reproduction number is computed, and it is shown to act as the key quantity that determines whether the disease continues inside the population. Finally, the local stability study indicates that the disease-free equilibrium stays locally asymptotically stable as long as the reproduction threshold is held strictly below one. The numerical investigations across different climate settings, show that rising temperature, higher rainfall intensity, and greater humidity tend to raise vector abundance and disease prevalence in a noticeable way. The sensitivity analysis, on the other hand, points out vector recruitment rate and climate- modified transmission coefficients as the leading drivers behind how quickly disease spreads. The results also show that using integrated vector management along with environmental sanitation, plus climate adaptive interventions, can substantially lower infection prevalence and the risk that outbreaks will happen. Overall, these findings give measurable evidence for reinforcing environmental health policies, and also for building climate adaptation strategies in the Niger-Delta region. The basic structure that was developed in this work serves as a practical decision support instrument, prepared for policymakers, public health agencies, and environmental regulators who are professionally engaged in prevention efforts and climate resilience planning.

**Keywords:** Climate Change, Vector-Borne Diseases, Environmental Health, Niger-Delta, Mathematical Modelling, Disease

## 1. Introduction

Vector- borne diseases are still among the biggest public health challenges facing developing countries. Per the World Health Organization, these infections make up a large slice of infectious diseases worldwide, and they drive hundreds of thousands of deaths each year. Malaria, dengue fever, yellow fever, chikungunya, Lassa fever, and multiple new zoonotic illnesses keep putting vulnerable communities at risk, especially in tropical and subtropical areas [1, 2]. Nigeria carries a serious share of illnesses that spread through vectors,

and malaria is still one of the main reasons for both sickness and death. The Niger Delta area is especially at risk, mainly due to its own particular environment. The results indicate big wetlands, mangrove forests, waterways, flood plains, and coastal systems that provide suitable breeding habitats for disease carriers. Since there is plenty of stagnant water, plus high humidity, and long rainy periods, vector survival is prolonged, and transmission keeps getting easier [3, 4].

Recent studies show that climate change is increasingly reshaping the epidemiology of vector-borne diseases worldwide. Higher temperatures can speed up vector development, tweak pathogen incubation periods, push biting activity upward, and also reduce or extend vector survival depending on conditions. At the same time, rainfall shifts shape the availability of breeding grounds, while humidity modulates vector lifespan and their dispersal capacity. So overall, climate variability ends up acting as a major driver for how strong transmission becomes, and whether outbreaks occur, again and again [5, 6].

The Niger–Delta region has experienced significant environmental changes in recent decades, including increased flooding, coastal erosion, sea-level rise, changing rainfall patterns, and rising temperatures. These climatic changes are further intensified by human activities such as oil exploration, gas flaring, urbanization, deforestation, and environmental pollution. Together, these factors increase human–vector interactions and create favourable conditions for disease emergence and persistence [7, 8].

Understanding the interactions among climate variables, vector ecology, and disease transmission requires analytical tools capable of capturing complex nonlinear dynamics. Mathematical modelling provides an effective framework for studying these relationships and evaluating potential intervention strategies. Differential equation models have been widely applied in epidemiology and have become valuable tools for public health planning and environmental management [9, 10].

Although several studies have investigated climate-driven disease transmission using compartmental models, many focus on generic settings and do not adequately capture the unique environmental characteristics of the Niger–Delta region. Furthermore, localized climate-sensitive vector dynamics and environmental disturbances remain insufficiently represented in many existing modelling frameworks, limiting their applicability to regional disease control planning and environmental health policy development [11, 12].

Motivated by these gaps, the present study develops a climate-sensitive host-vector model tailored to the environmental and climatic conditions of the Niger Delta region. Within a unified mathematical framework, it brings together climate- dependent transmission effects along with vector population dynamics, and both are treated together, not separately. The overall aim is to see, quantitatively, how changes in temperature, rainfall, and relative humidity steer disease transmission. At the same time, it identifies potential intervention strategies that could meaningfully reduce the disease burden, even when the climatic conditions keep changing.

These findings add to the expanding knowledge base on climate-sensitive epidemiological modelling by providing a solid mathematical framework for understanding how climate variability connects with vector-borne transmission. Also, the work provides practical pointers for decision-makers, environmental managers, public health officials, and other groups involved in prevention efforts, environmental stewardship, and resilience planning. In the long run, the proposed framework can function as a decision-support instrument, useful for designing interventions that are useful and for supporting sustainable public health outcomes, especially in regions that are climate-vulnerable.

## 2. Model Formulation and Structure

To investigate the influence of climate change on vector-borne disease transmission in the Niger–Delta region, a climate-sensitive host–vector epidemiological model is developed. The model incorporates interactions between human and vector populations while explicitly accounting for the effects of environmental variables such as temperature, rainfall, and humidity on disease transmission and vector population dynamics. The incorporation of climate-related factors into epidemiological models has become increasingly important due to growing evidence that environmental variability significantly influences disease emergence, transmission patterns, and public health outcomes [16, 17].

The total human population at time $t$, represented by $N_h(t)$, is partitioned into four mutually exclusive epidemiological classes comprising susceptible $\big(S_h(t)\big)$, exposed $\big(E_h(t)\big)$, infectious $\big(I_h(t)\big)$, and recovered $\big(R_h(t)\big)$ individuals. Accordingly, the total human population satisfies:

$$N_h(t) = S_h(t) + E_h(t) + I_h(t) + R_h(t). \tag{1}$$

The vector population at time $t$, represented by $N_v(t)$, is partitioned into three mutually exclusive epidemiological classes comprising susceptible vectors $\big(S_v(t)\big)$, exposed vectors $\big(E_v(t)\big)$, and infectious vectors $\big(I_v(t)\big)$. Consequently, the total vector population is given by

$$N_v(t) = S_v(t) + E_v(t) + I_v(t). \tag{2}$$

The model assumes that disease transmission occurs through contacts between susceptible humans and infectious vectors, as well as between susceptible vectors and infectious humans. Climate variability influences vector recruitment, survival, biting rates, and transmission efficiency.

Let $T(t)$, $R(t)$, and $H(t)$ denote the ambient temperature, rainfall intensity, and relative humidity at time $t$, respectively. Since climatic conditions directly influence vector abundance, survival, and disease transmission, the transmission coefficient is assumed to depend explicitly on these environmental variables. Accordingly, the climate-dependent transmission coefficient is defined as

$$\beta(T,R,H)=\beta_0\begin{Bmatrix}1+a_T(T-T_0)\\ +a_R(R-R_0)\\ +a_H(H-H_0)\end{Bmatrix}. \tag{3}$$

where $\beta_0$ denotes the baseline transmission coefficient under the reference climatic conditions $(T_0, R_0, H_0)$, with $T_0$, $R_0$, and $H_0$ representing the baseline temperature, rainfall, and relative humidity, respectively. The parameters $a_T$, $a_R$, and $a_H$ are non-negative climate sensitivity coefficients, they quantify the effects of temperature, rainfall, and humidity on disease transmission. If $a_T$ $a_R$, or $a_H$ come out larger, then the climatic impact on transmission intensity is stronger. If they are smaller, the the influence of environmental variability is reduced for how the disease spreads, or at least that influence is weaker.

The recruitment and survival of disease vectors are similarly affected by prevailing environmental conditions. To incorporate the effects of climate variability on vector population dynamics, the vector recruitment rate is modeled as a climate-dependent function of temperature, rainfall, and relative humidity. Accordingly, the vector recruitment function is defined as

$$\Lambda_v(T,R,H)=\Lambda_{v0}\begin{Bmatrix}1+b_T(T-T_0)\\ +b_R(R-R_0)\\ +b_H(H-H_0)\end{Bmatrix}, \tag{4}$$

where $\Lambda_{v0}$ denotes the baseline vector recruitment rate under the reference climatic conditions, while $b_T$, $b_R$, and $b_H$ are climate-sensitivity parameters that measure the effects of temperature, rainfall, and humidity on vector reproduction, development, and survival. Positive values of these parameters imply that favourable climatic conditions enhance vector recruitment and population growth, thereby increasing the potential for disease transmission.

Incorporating the climate-dependent transmission and vector recruitment functions, the transmission dynamics of the climate-sensitive host–vector disease system are governed by the following system of nonlinear ordinary differential equations:

$$\begin{cases}\dfrac{dS_h}{dt}=\Lambda_h-\dfrac{\beta_{hv}(T,R,H)S_hI_v}{N_h}-\mu_hS_h,\\ \dfrac{dE_h}{dt}=\dfrac{\beta_{hv}(T,R,H)S_hI_v}{N_h}-(\sigma_h+\mu_h)E_h,\\ \dfrac{dI_h}{dt}=\sigma_hE_h-(\gamma_h+\delta_h+\mu_h)I_h,\\ \dfrac{dR_h}{dt}=\gamma_hI_h-\mu_hR_h,\\ \dfrac{dS_v}{dt}=\Lambda_v(T,R,H)-\dfrac{\beta_{vh}(T,R,H)S_vI_h}{N_h}-\mu_vS_v,\\ \dfrac{dE_v}{dt}=\dfrac{\beta_{vh}(T,R,H)S_vI_h}{N_h}-(\sigma_v+\mu_v)E_v,\\ \dfrac{dI_v}{dt}=\sigma_vE_v-\mu_vI_v.\end{cases} \tag{5}$$

System (5) describes the coupled transmission dynamics between the human and vector populations under the influence of climatic variability. The human population is replenished through recruitment at a constant rate $\Lambda_h$, while susceptible individuals become exposed following effective contact with infectious vectors. Individuals in the exposed class undergo a latent period before progressing to the infectious class at rate $\sigma_h$. Infectious individuals either recover and move to the recovered class at rate $\gamma_h$ or leave the infectious class through disease-induced mortality at rate $\delta_h$ and natural mortality at rate $\mu_h$. Recovered individuals are assumed to acquire temporary immunity and are subject only to natural mortality. Such compartmental representations have been widely employed in epidemiological studies to characterize disease-transmission processes, estimate key epidemiological parameters, and evaluate the effects of environmental variability on outbreak dynamics [18-20].

The vector population is recruited according to the climate-dependent function $\Lambda_v(T,R,H)$, which captures the influence of temperature, rainfall, and relative humidity on vector reproduction, development, and survival. Susceptible vectors acquire infection through contact with infectious humans and subsequently enter the exposed class. Following an incubation period, exposed vectors progress to the infectious class at rate $\sigma_v$. Since recovery is generally not assumed for disease vectors, infectious vectors remain capable of transmitting the infection throughout their lifespan until death occurs at rate $\mu_v$.

Consequently, the proposed model captures the combined effects of climatic variability and host–vector interactions on disease transmission dynamics, thereby providing a mathematical framework for assessing the impact of climate change on vector-borne disease prevalence and persistence in the Niger–Delta region.

### *2.1. Basic Model Assumptions*

The formulation of the model is based on the following assumptions. The human population is assumed to mix homogeneously within the study region. Disease transmission occurs exclusively through vector-host interactions. Climatic variables influence transmission rates and vector recruitment but do not directly affect human recovery. Recovered humans acquire temporary immunity during the study period. Vector populations respond rapidly to environmental changes in temperature, rainfall, and humidity. All model parameters are assumed to be nonnegative constants except for the climate-dependent transmission and recruitment functions.

### *2.2. Description of Model Parameters*

The state variables and parameters employed in the proposed climate-sensitive host–vector disease model are summarized in Table 1.

***Table 1.*** *Model parameters, descriptions, and units.*

| Parameter | Description | Unit |
|---|---|---|
| $\Lambda_h$ | Human recruitment rate | persons/day |
| $\mu_h$ | Human mortality rate | day$^{-1}$ |
| $\sigma_h$ | Human incubation rate | day$^{-1}$ |
| $\gamma_h$ | Human recovery rate | day$^{-1}$ |
| $\delta_h$ | Disease mortality rate | day$^{-1}$ |
| $\Lambda_{v0}$ | Baseline vector recruitment rate | vectors/day |
| $\mu_v$ | Vector mortality rate | day$^{-1}$ |
| $\sigma_v$ | Vector incubation rate | day$^{-1}$ |
| $\beta_{hv}$ | Vector–human transmission rate | day$^{-1}$ |
| $\beta_{vh}$ | Human–vector transmission rate | day$^{-1}$ |
| $T(t)$ | Temperature | °C |
| $R(t)$ | Rainfall intensity | rainfall-unit |
| $H(t)$ | Relative humidity | % |
| $a_T$ | Temperature sensitivity coefficient | °C$^{-1}$ |
| $a_R$ | Rainfall sensitivity coefficient | rainfall-unit$^{-1}$ |
| $a_H$ | Humidity sensitivity coefficient | %$^{-1}$ |
| $b_T$ | Temperature recruitment sensitivity coefficient | °C$^{-1}$ |
| $b_R$ | Rainfall recruitment sensitivity coefficient | rainfall-unit$^{-1}$ |
| $b_H$ | Humidity recruitment sensitivity coefficient | %$^{-1}$ |

The model developed in this section provides a mathematical framework for investigating the influence of climate variability on vector population dynamics and disease transmission in the Niger–Delta region. The next section establishes the fundamental mathematical properties of the model, including existence and uniqueness of solutions, positivity, boundedness, equilibrium analysis, and stability conditions. “‘

# 3. Mathematical Analysis of the Model

This section establishes the fundamental mathematical properties of the climate-sensitive vector-borne disease model developed in Section 2. Specifically, the existence and uniqueness of solutions, positivity of solutions, boundedness of model trajectories, invariant region, disease-free equilibrium, endemic equilibrium, and the basic reproduction number are investigated. These analyses ensure that the model is mathematically well-posed and epidemiologically meaningful. Such theoretical investigations are essential for guaranteeing the biological validity of epidemiological models and for establishing rigorous stability conditions governing disease transmission dynamics [20-26].

### *3.1. Existence and Uniqueness of the Model-Solutions*

Let

$$X(t) = (S_h, E_h, I_h, R_h, S_v, E_v, I_v)^T. \tag{6}$$

Then, system (5) can be written compactly as

$$\frac{dX}{dt} = F(X), \tag{7}$$

where (F(X)) is continuously differentiable in the biologically feasible region

$$\Omega = \mathbb{R}^7_+. \tag{8}$$

*Theorem* 3.1. For every nonnegative initial condition $X(0) \in \mathbb{R}^7_+$, system (5) admits a unique solution on $[0, \infty)$.

*Proof*

The right-hand sides of system (5) are continuously differentiable with respect to the state variables. So the vector field $F(X)$ satisfies the local Lipschitz condition on $\mathbb{R}^7_+$, because of the Picard-Lindelöf Theorem, there exists a unique local solution for each nonnegative initial condition. Now, since the solutions remain bounded inside the biologically feasible region, that local trajectory can be pushed forward in time, and it extends uniquely over the whole interval $[0, \infty)$. Hence system (5) has one and only one global solution. □

### *3.2. Positivity of Solutions*

For epidemiological validity, all state variables must remain nonnegative for all time.

*Theorem* 3.2. If the initial conditions are nonnegative, then all solutions of system (5) remain nonnegative for all $t \geq 0$.

*Proof*

Consider the susceptible human compartment:

$$\frac{dS_h}{dt} = \Lambda_h - \frac{\beta_{hv}(T,R,H)S_h I_v}{N_h} - \mu_h S_h. \tag{9}$$

At $S_h = 0$,

$$\frac{dS_h}{dt}\Big|_{S_h=0} = \Lambda_h > 0. \tag{10}$$

Similarly,

$$\frac{dE_h}{dt}\Big|_{E_h=0} = \frac{\beta_{hv}(T,R,H)S_h I_v}{N_h} \geq 0, \tag{11}$$

$$\frac{dI_h}{dt}\Big|_{I_h=0} = \sigma_h E_h \geq 0, \tag{12}$$

and

$$\frac{dR_h}{dt}\Big|_{R_h=0} = \gamma_h I_h \geq 0. \tag{13}$$

Likewise, for the vector population,

$$\frac{dS_v}{dt}\Big|_{S_v=0} = \Lambda_v(T,R,H) \geq 0, \tag{14}$$

$$\frac{dE_v}{dt}\Big|_{E_v=0} = \frac{\beta_{vh}(T,R,H)S_v I_h}{N_h} \geq 0, \tag{15}$$

and

$$\frac{dI_v}{dt}\Big|_{I_v=0} = \sigma_v E_v \geq 0. \tag{16}$$

Hence, no solution trajectory can cross any coordinate hyperplane into the negative orthant. So, all state variables remain nonnegative for all $t \geq 0$.

Consequently, the nonnegative orthant $\mathbb{R}^7_+$ is positively invariant under the flow of system (5). □

### *3.3. Boundedness of Solutions and Invariant Region*

To establish the boundedness of solutions, consider the total human population

$$N_h = S_h + E_h + I_h + R_h. \tag{17}$$

Adding the first four equations of system (5) gives

$$\frac{dN_h}{dt} = \Lambda_h - \mu_h N_h - \delta_h I_h. \tag{18}$$

Since $\delta_h I_h \geq 0$, it follows that

$$\frac{dN_h}{dt} \leq \Lambda_h - \mu_h N_h. \tag{19}$$

Applying the Comparison Theorem yields

$$N_h(t) \leq \frac{\Lambda_h}{\mu_h} + \left(N_h(0) - \frac{\Lambda_h}{\mu_h}\right) e^{-\mu_h t}. \tag{20}$$

Hence,

$$0 \leq N_h(t) \leq \frac{\Lambda_h}{\mu_h}. \tag{21}$$

Similarly, let

$$N_v = S_v + E_v + I_v \tag{22}$$

denote the total vector population. Summing the last three equations of system (5) gives

$$\frac{dN_v}{dt} = \Lambda_v(T, R, H) - \mu_v N_v. \tag{23}$$

Therefore,

$$0 \leq N_v(t) \leq \frac{\Lambda_v^{\max}}{\mu_v}, \tag{24}$$

where

$$\Lambda_v^{\max} = \max\left\{\Lambda_v(T, R, H)\right\}. \tag{25}$$

Consequently, the feasible region

$$\Omega = \left\{ X \in \mathbb{R}_+^7 : N_h \leq \frac{\Lambda_h}{\mu_h},\ N_v \leq \frac{\Lambda_v^{\max}}{\mu_v} \right\} \tag{26}$$

is positively invariant and attracting.

Therefore, all solutions of system (5) that originate in $\Omega$ remain in $\Omega$ for all $t \geq 0$. Hence, the model is epidemiologically and mathematically well posed.

### *3.4. Disease-Free Equilibrium*

The disease-free equilibrium (DFE) corresponds to the state in which no infection exists in either the human or vector population.

Setting

$$E_h = I_h = R_h = E_v = I_v = 0 \tag{27}$$

in system (5) and solving the resulting steady-state equations yield

$$S_h^0 = \frac{\Lambda_h}{\mu_h}, \tag{28}$$

and

$$S_v^0 = \frac{\Lambda_v(T, R, H)}{\mu_v}. \tag{29}$$

Therefore, the disease-free equilibrium is given by

$$E_0 = \left(\frac{\Lambda_h}{\mu_h}, 0, 0, 0, \frac{\Lambda_v(T, R, H)}{\mu_v}, 0, 0\right). \tag{30}$$

The disease-free equilibrium implies a state in which the disease has been entirely eliminated from both the human and vector populations. Consequently, all individuals in the population are susceptible, and no active transmission occurs within the system.

### *3.5. Basic Reproduction Number*

The basic reproduction number, denoted by $R_0$, represents the expected number of secondary infections generated by a typical infectious individual introduced into a completely susceptible population. It serves as a threshold parameter for determining whether disease transmission can invade and persist in the population.

Using the next-generation matrix approach, the infected compartments are taken as

$$\mathbf{z} = (E_h, I_h, E_v, I_v)^T. \tag{31}$$

At the disease-free equilibrium

$$E_0 = \left(S_h^0, 0, 0, 0, S_v^0, 0, 0\right),$$

where

$$S_h^0 = \frac{\Lambda_h}{\mu_h}, \qquad S_v^0 = \frac{\Lambda_v(T, R, H)}{\mu_v}, \tag{32}$$

and

$$N_h^0 = S_h^0.$$

The infected subsystem of system (5) can be decomposed as

$$\dot{\mathbf{z}} = \mathcal{F}(\mathbf{z}) - \mathcal{V}(\mathbf{z}),$$

where $\mathcal{F}$ contains the rates of appearance of new infections, while $\mathcal{V}$ contains all other transfers into and out of the infected compartments.

Linearizing these terms about $E_0$, the transmission matrix is

$$F = \begin{pmatrix} 0 & 0 & 0 & \dfrac{\beta_{hv}(T, R, H) S_h^0}{N_h^0} \\ 0 & 0 & 0 & 0 \\ 0 & \dfrac{\beta_{vh}(T, R, H) S_v^0}{N_h^0} & 0 & 0 \\ 0 & 0 & 0 & 0 \end{pmatrix}. \tag{33}$$

The transition matrix is

$$V = \begin{pmatrix} \sigma_h + \mu_h & 0 & 0 & 0 \\ -\sigma_h & \gamma_h + \delta_h + \mu_h & 0 & 0 \\ 0 & 0 & \sigma_v + \mu_v & 0 \\ 0 & 0 & -\sigma_v & \mu_v \end{pmatrix}. \tag{34}$$

The next-generation matrix is therefore

$$K = FV^{-1}. \tag{35}$$

For convenience, define

$$A_h = \sigma_h + \mu_h, \qquad B_h = \gamma_h + \delta_h + \mu_h,$$

and

$$A_v = \sigma_v + \mu_v.$$

Then

$$V^{-1} = \begin{pmatrix} \frac{1}{A_h} & 0 & 0 & 0 \\ \frac{\sigma_h}{A_h B_h} & \frac{1}{B_h} & 0 & 0 \\ 0 & 0 & \frac{1}{A_v} & 0 \\ 0 & 0 & \frac{\sigma_v}{A_v \mu_v} & \frac{1}{\mu_v} \end{pmatrix}. \tag{36}$$

Consequently,

$$K = \begin{pmatrix} 0 & 0 & \frac{\beta_{hv} S_h^0 \sigma_v}{N_h^0 A_v \mu_v} & \frac{\beta_{hv} S_h^0}{N_h^0 \mu_v} \\ 0 & 0 & 0 & 0 \\ \frac{\beta_{vh} S_v^0 \sigma_h}{N_h^0 A_h B_h} & \frac{\beta_{vh} S_v^0}{N_h^0 B_h} & 0 & 0 \\ 0 & 0 & 0 & 0 \end{pmatrix}. \tag{37}$$

The basic reproduction number is given by the spectral radius of the next-generation matrix:

$$R_0 = \rho(K) = \rho(FV^{-1}). \tag{38}$$

The nonzero eigenvalues associated with the transmission cycle are determined by the product of the human-to-vector and vector-to-human transmission pathways. Hence,

$$R_0 = \left[ \frac{\beta_{hv}(T,R,H)\beta_{vh}(T,R,H) S_h^0 S_v^0 \sigma_h \sigma_v}{N_h^{0\,2}(\sigma_h + \mu_h)(\gamma_h + \delta_h + \mu_h)(\sigma_v + \mu_v)\mu_v} \right]^{1/2}. \tag{39}$$

Since

$$S_h^0 = \frac{\Lambda_h}{\mu_h}, \qquad S_v^0 = \frac{\Lambda_v(T,R,H)}{\mu_v},$$

substitution into (39) gives

$$R_0 = \left[ \frac{\beta_{hv}(T,R,H)\beta_{vh}(T,R,H)\Lambda_h \Lambda_v(T,R,H)\sigma_h \sigma_v}{\mu_h \mu_v^2 N_h^{0\,2}(\sigma_h + \mu_h)(\gamma_h + \delta_h + \mu_h)(\sigma_v + \mu_v)} \right]^{1/2}. \tag{40}$$

Thus, $R_0$ depends explicitly on the climate-sensitive transmission coefficients and the vector recruitment function $\Lambda_v(T,R,H)$. Consequently, climatic conditions that increase vector recruitment or transmission efficiency may raise $R_0$, thereby increasing the potential for disease invasion and persistence. Conversely, interventions that reduce vector recruitment and transmission can decrease $R_0$ below unity, favouring disease elimination.

Equation (40) shows that the basic reproduction number depends explicitly on the climate-sensitive vector recruitment function $\Lambda_v(T,R,H)$. Consequently, climatic conditions that enhance vector recruitment, survival, and transmission efficiency may increase the value of $R_0$, thereby facilitating disease invasion and persistence. Conversely, environmental and public health interventions that reduce vector abundance and transmission rates can lower $R_0$ below unity, leading to disease elimination.

### *3.6. Local Stability of the Disease-Free Equilibrium*

The local stability of the disease-free equilibrium $E_0$ is determined using the basic reproduction number $R_0$.

*Theorem* 3.3. The disease-free equilibrium $E_0$ is locally asymptotically stable whenever $R_0 < 1$ and unstable whenever $R_0 > 1$.

*Proof*

Linearizing system (5) about the disease-free equilibrium $E_0$ yields the Jacobian matrix $J(E_0)$. The eigenvalues corresponding to the uninfected compartments are strictly negative, while those associated with the infected subsystem are determined by the next-generation matrix.

By the next-generation matrix method, the spectral radius of $FV^{-1}$ is given by $R_0$. Consequently, all eigenvalues of $J(E_0)$ have negative real parts whenever $R_0 < 1$. Hence, the disease-free equilibrium is locally asymptotically stable. Conversely, if $R_0 > 1$, at least one eigenvalue has a positive real part, and therefore $E_0$ becomes unstable. □

### *3.7. Global Stability of the Disease-Free Equilibrium*

*Theorem* 3.4. Let

$$E_0 = \left(S_h^0, 0, 0, 0, S_v^0, 0, 0\right)$$

denote the disease-free equilibrium of system (5), where

$$S_h^0 = \frac{\Lambda_h}{\mu_h}, \qquad S_v^0 = \frac{\Lambda_v(T,R,H)}{\mu_v}.$$

For fixed climatic conditions $(T,R,H)$, if $R_0 < 1$, and the infected subsystem satisfies the standard comparison condition with its linearization at $E_0$ then $E_0$ is globally asymptotically stable in the feasible region $\Omega$.

*Proof.* Let

$$\mathbf{z} = (E_h, I_h, E_v, I_v)^T$$

denote the vector of infected compartments. The infected subsystem can be written in the form

$$\dot{\mathbf{z}} = [F(\mathbf{x}) - V]\,\mathbf{z},$$

where $F(\mathbf{x})$ represents the matrix of new infections and $V$ represents the transition and removal terms.

At the disease-free equilibrium, the next-generation matrix is

$$K = F_0 V^{-1},$$

where $F_0 = F(E_0)$. Hence, the basic reproduction number is

$$R_0 = \rho(F_0 V^{-1}),$$

where $\rho(\cdot)$ denotes the spectral radius.

Since $R_0 < 1$, the matrix $F_0 - V$ is stable. Therefore, there exists a positive vector

$$w = (w_1, w_2, w_3, w_4)^T > 0$$

such that

$$w^T(F_0 - V) < 0.$$

Consider the Lyapunov function

$$L(\mathbf{z}) = w_1 E_h + w_2 I_h + w_3 E_v + w_4 I_v.$$

Clearly,

$$L(\mathbf{z}) \geq 0,$$

with equality if and only if

$$E_h = I_h = E_v = I_v = 0.$$

Along the solutions of system (5),

$$\begin{aligned} \dot{L} &= w^T \dot{\mathbf{z}} \\ &\leq w^T(F_0 - V)\mathbf{z} \\ &< 0, \end{aligned}$$

for every $\mathbf{z} \neq 0$ in $\Omega$.

Consequently,

$$E_h(t),\ I_h(t),\ E_v(t),\ I_v(t) \longrightarrow 0 \qquad \text{as } t \to \infty.$$

Thus, the infected compartments vanish asymptotically, while the remaining compartments converge to their disease-free equilibrium values. By LaSalle's invariance principle, the largest invariant set contained in

$$\{\mathbf{z} \in \Omega : \dot{L} = 0\}$$

is the singleton $\{E_0\}$. Hence,

$$\boxed{E_0 \text{ is globally asymptotically stable whenever } R_0 < 1.}$$

*Theorem* 3.5. Let

$$E^* = (S_h^*, E_h^*, I_h^*, R_h^*, S_v^*, E_v^*, I_v^*)$$

denote an endemic equilibrium of system (5). For fixed climatic conditions $(T, R, H)$, if

$$R_0 > 1,$$

then system (5) admits a positive endemic equilibrium, provided the equilibrium equations satisfy the positivity conditions stated below.

*Proof.* At equilibrium, define the forces of infection by

$$\lambda_h^* = \frac{\beta_{hv} I_v^*}{N_h^*}, \qquad \lambda_v^* = \frac{\beta_{vh} I_h^*}{N_h^*},$$

where

$$N_h^* = S_h^* + E_h^* + I_h^* + R_h^*.$$

From the equilibrium equations,

$$S_h^* = \frac{\Lambda_h}{\mu_h + \lambda_h^*},$$

$$E_h^* = \frac{\lambda_h^* S_h^*}{\sigma_h + \mu_h},$$

$$I_h^* = \frac{\sigma_h \lambda_h^* S_h^*}{(\sigma_h + \mu_h)(\gamma_h + \delta_h + \mu_h)},$$

and

$$R_h^* = \frac{\gamma_h I_h^*}{\mu_h}.$$

Similarly, for the vector population,

$$S_v^* = \frac{\Lambda_v(T, R, H)}{\mu_v + \lambda_v^*},$$

$$E_v^* = \frac{\lambda_v^* S_v^*}{\sigma_v + \mu_v},$$

and

$$I_v^* = \frac{\sigma_v \lambda_v^* S_v^*}{\mu_v(\sigma_v + \mu_v)}.$$

Define

$$c_h = \frac{\sigma_h}{(\sigma_h + \mu_h)(\gamma_h + \delta_h + \mu_h)}$$

and

$$c_v = \frac{\sigma_v}{\mu_v(\sigma_v + \mu_v)}.$$

Then

$$I_h^* = c_h \lambda_h^* S_h^*$$

and

$$I_v^* = c_v \lambda_v^* S_v^*.$$

Using the definitions of $\lambda_h^*$ and $\lambda_v^*$ gives

$$\lambda_v^* = \frac{\beta_{vh} c_h \lambda_h^* S_h^*}{N_h^*}$$

and

$$\lambda_h^* = \frac{\beta_{hv} c_v \lambda_v^* S_v^*}{N_h^*}.$$

For $\lambda_h^* > 0$, these relations can be reduced to a scalar equilibrium equation

$$\Phi(\lambda_h^*) = 1,$$

where $\Phi$ is a continuous function on the positive interval determined by the feasible region.

At the disease-free state,

$$\lim_{\lambda_h \to 0^+} \Phi(\lambda_h) = R_0^2.$$

Hence, if

$$R_0 > 1,$$

then

$$\lim_{\lambda_h \to 0^+} \Phi(\lambda_h) > 1.$$

On the other hand, as the force of infection increases within the feasible region,

$$\lim_{\lambda_h \to \infty} \Phi(\lambda_h) < 1.$$

By the intermediate value theorem, there exists

$$\lambda_h^* > 0$$

such that

$$\Phi(\lambda_h^*) = 1.$$

Consequently,

$$S_h^*,\ E_h^*,\ I_h^*,\ R_h^*,\ S_v^*,\ E_v^*,\ I_v^* > 0.$$

Therefore, system (5) admits a positive endemic equilibrium whenever

$$\boxed{R_0 > 1.}$$

*Theorem* 3.6. Let

$$E^* = (S_h^*, E_h^*, I_h^*, R_h^*, S_v^*, E_v^*, I_v^*)$$

be a positive endemic equilibrium of system (5). Suppose that $R_0 > 1$. The endemic equilibrium $E^*$ is locally asymptotically stable if the characteristic polynomial of the Jacobian matrix $J(E^*)$ satisfies the Routh–Hurwitz stability conditions.

*Proof.* Let $J(E^*)$ denote the Jacobian matrix of system (5) evaluated at the endemic equilibrium $E^*$. The linearized system in a neighbourhood of $E^*$ is given by

$$\dot{\mathbf{u}} = J(E^*)\mathbf{u},$$

where

$$\mathbf{u} = \begin{pmatrix} S_h - S_h^* \\ E_h - E_h^* \\ I_h - I_h^* \\ R_h - R_h^* \\ S_v - S_v^* \\ E_v - E_v^* \\ I_v - I_v^* \end{pmatrix}.$$

The characteristic equation associated with $J(E^*)$ is

$$\det\left(\lambda I - J(E^*)\right) = 0.$$

Hence, the characteristic polynomial can be written as

$$P(\lambda) = \lambda^7 + a_1\lambda^6 + a_2\lambda^5 + a_3\lambda^4 + a_4\lambda^3 + a_5\lambda^2 + a_6\lambda + a_7. \quad (41)$$

The corresponding Routh–Hurwitz matrix is

$$\mathcal{R} = \begin{pmatrix} a_1 & a_3 & a_5 & a_7 & 0 & 0 & 0 \\ 1 & a_2 & a_4 & a_6 & 0 & 0 & 0 \\ 0 & a_1 & a_3 & a_5 & a_7 & 0 & 0 \\ 0 & 1 & a_2 & a_4 & a_6 & 0 & 0 \\ 0 & 0 & a_1 & a_3 & a_5 & a_7 & 0 \\ 0 & 0 & 1 & a_2 & a_4 & a_6 & 0 \\ 0 & 0 & 0 & a_1 & a_3 & a_5 & a_7 \end{pmatrix}. \quad (42)$$

Let $\Delta_k$ denote the determinant of the leading $k \times k$ principal submatrix of the Routh–Hurwitz matrix $R$, that is,

$$\Delta_k = \det(R_k), \qquad k = 1, 2, \ldots, 7.$$

By the Routh–Hurwitz criterion, the characteristic polynomial

$$P(\lambda) = \lambda^7 + a_1\lambda^6 + a_2\lambda^5 + a_3\lambda^4 + a_4\lambda^3 + a_5\lambda^2 + a_6\lambda + a_7$$

has all its roots in the open left half-plane if and only if

$$\Delta_k > 0, \qquad k = 1, 2, \ldots, 7.$$

Hence, whenever these seven Routh–Hurwitz determinants are positive, all eigenvalues of $J(E^*)$ have negative real parts. Consequently, the endemic equilibrium $E^*$ is locally asymptotically stable.

By the Routh–Hurwitz criterion, all roots of the characteristic polynomial (41) have negative real parts if

$$\Delta_k > 0, \qquad k = 1, 2, \ldots, 7. \quad (43)$$

Under condition (43), every eigenvalue of $J(E^*)$ has a negative real part. Therefore, the endemic equilibrium $E^*$ is locally asymptotically stable.

Hence,

$$\boxed{E^* \text{ is locally asymptotically stable if } \Delta_k > 0, \quad k = 1, \ldots, 7.}$$

For the present parameterization, the numerical scenarios considered in Section 4 satisfy $R_0 < 1$. Consequently, they do not generate a positive endemic equilibrium at which the Routh–Hurwitz determinants can be numerically evaluated. The stability result in Theorem 3.6 is therefore stated as a conditional analytical result for parameter regimes satisfying $R_0 > 1$ and the Routh–Hurwitz conditions. Numerical evaluation of the determinants for an endemic-equilibrium parameter regime is left for future investigation.

### *3.8. Climate Threshold Analysis*

The basic reproduction number $R_0$ serves as a critical threshold parameter governing the long-term dynamics of the disease within the population. Since both the climate-dependent transmission coefficient $\beta(T, R, H)$ and the vector recruitment function $\Lambda_v(T, R, H)$ depend explicitly on temperature, rainfall, and relative humidity, variations in these climatic factors directly influence the magnitude of $R_0$.

From the expression for $R_0$, it follows that favourable climatic conditions that enhance vector breeding, survival, and transmission efficiency increase the value of $R_0$. On the other hand, harsh environmental circumstances reduce how many vectors are recruited and also how intensely transmission happens, so, in the end $R_0$ decreases.

As a result, climate variability can reshape disease dynamics by moving the system past the epidemiological tipping point where $R_0 = 1$. If $R_0 > 1$, the disease can invade and keep going, and this means an endemic state will become established. Conversely, when $R_0 < 1$, disease transmission cannot be maintained, and the infection will eventually die out.

### 3.9. Sensitivity Analysis of the Basic Reproduction Number

To identify the most influential parameters on the spreading, a normalized forward sensitivity analysis is performed on the basic reproduction number to quantify the influence of each parameter how each factor affects it.

The normalized sensitivity index of $R_0$ with respect to a parameter $p$ is defined by

$$S_p^{R_0} = \frac{\partial R_0}{\partial p} \cdot \frac{p}{R_0}. \tag{44}$$

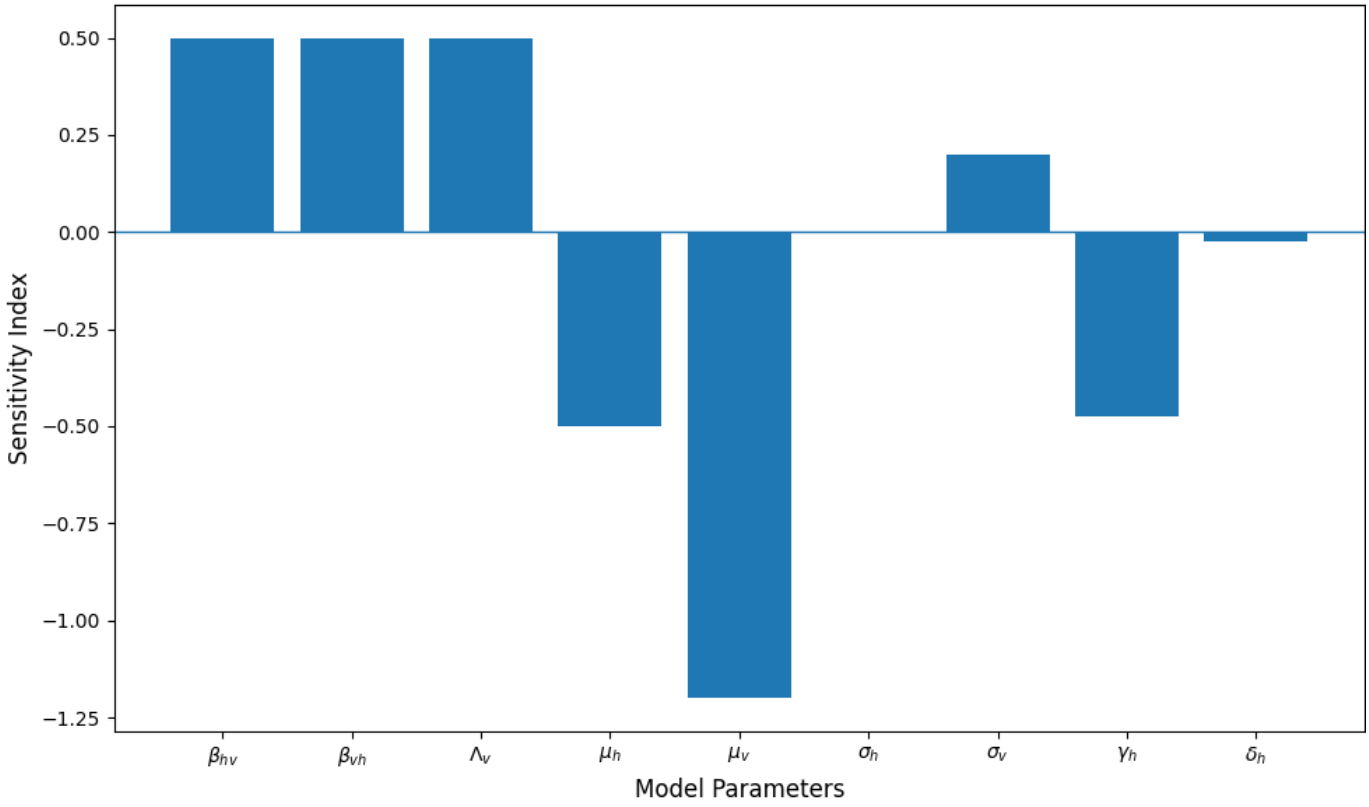


***Figure 1.*** *Sensitivity Analysis of the Basic Reproduction Number.*

Figure 1 and Table 2 present the normalized sensitivity indices of $R_0$ and their corresponding rankings. The results show that $\mu_v$ has the largest absolute influence on $R_0$, while $\beta_{hv}$, $\beta_{vh}$, and $\Lambda_v$ have positive sensitivity indices, indicating increased transmission potential. In contrast, $\mu_h$ and $\mu_v$ have negative sensitivity indices, indicating that increased mortality reduces $R_0$. These results identify vector mortality, recruitment, and transmission rates as important parameters for disease control.

From the expression for $R_0$, the sensitivity indices of the principal parameters are obtained as

$$S_{\beta_{hv}}^{R_0} = S_{\beta_{vh}}^{R_0} = S_{\Lambda_v}^{R_0} = \frac{1}{2}, \tag{45}$$

$$S_{\mu_h}^{R_0} = -\frac{1}{2}\left(1 + \frac{\mu_h}{\sigma_h + \mu_h}\right), \tag{46}$$

and

$$S_{\mu_v}^{R_0} = -\frac{1}{2}\left(2 + \frac{\mu_v}{\sigma_v + \mu_v}\right). \tag{47}$$

***Table 2.*** *Normalized sensitivity indices and ranking of model parameters with respect to the basic reproduction number $R_0$.*

| Parameter | Sensitivity Index | Rank |
|---|---|---|
| $\mu_v$ | $-1.2000$ | 1 |
| $\beta_{hv}$ | $+0.5000$ | 2 |
| $\beta_{vh}$ | $+0.5000$ | 2 |
| $\Lambda_v$ | $+0.5000$ | 2 |
| $\mu_h$ | $-0.5001$ | 5 |
| $\gamma_h$ | $-0.4760$ | 6 |
| $\sigma_v$ | $+0.2000$ | 7 |
| $\delta_h$ | $-0.0238$ | 8 |
| $\sigma_h$ | $+0.0001$ | 9 |

The sensitivity index captures the relative change in $R_0$ brought about by a relative change in a parameter $p$. If the sensitivity index is positive, then raising $p$ increases $R_0$. If it is negative, then increasing $p$ leads to a decrease in $R_0$.

For the proposed model, the transmission coefficients $\beta_{hv}$ and $\beta_{vh}$, along with the climate dependent vector recruitment function $\Lambda_v(T, R, H)$ are expected to have positive sensitivity

indices, because increases in these quantities will make disease spread more likely. Meanwhile, the mortality parameters $\mu_h$ and $\mu_v$ typically show negative sensitivity indices. This happens because higher mortality weakens the effective infectious period in humans and reduces vector survival. as a result, disease persistence is suppressed.

Overall, the sensitivity analysis gives valuable insights into how much epidemiological factors and climate-sensitive parameters each contribute to disease spread dynamics. The analysis identifies which parameters are the most influential for the basic reproduction number $R_0$, so it flags the key targets for action or prevention. This kind of information can help policymakers and public health authorities decide what to do first, using the more effective control approaches to reduce transmission and also to reduce the total disease burden.

In the present numerical analysis, the climatic variables $T(t)$, $R(t)$, and $H(t)$ are treated as fixed values within each simulation scenario. Thus, each scenario represents a specified climatic condition, such as baseline, increased temperature, increased rainfall, increased humidity, or combined climate change. The numerical experiments therefore constitute a scenario-based climate sensitivity analysis rather than simulations driven by continuously varying climatic time-series data.

# 4. Numerical Simulations and Scenario Analysis

This part presents the numerical simulations of the climate-sensitive, vector- borne disease model that was made in the earlier sections. The goal is to look at how climate variability changes disease spread dynamics and also to check how well climate-adaptive intervention strategies work, especially in the Niger-Delta region. The numerical findings, you can say, support the earlier theoretical work, and they give a useful perspective on how weather conditions link up with vector abundance and overall disease levels.

The nonlinear differential equation system was tackled numerically, using the standard fourth-order Runge-Kutta, often called RK4, approach as it was coded in Python. The simulations ran for 365 days, which stands for a full yearly transmission cycle. The parameter choices came from relevant epidemiological papers, and then they were tuned a bit so they match the climatic and ecological realities of the Niger-Delta area.

## *4.1. Baseline Parameter Values*

***Table 3.*** *Baseline parameter values and units used for numerical simulations.*

| Parameter | Description | Value | Unit |
|---|---|---|---|
| $\Lambda_h$ | Human recruitment | 50 | persons/day |
| $\mu_h$ | Human mortality | 0.00004 | day$^{-1}$ |
| $\sigma_h$ | Human incubation | 0.14 | day$^{-1}$ |
| $\gamma_h$ | Human recovery | 0.10 | day$^{-1}$ |
| $\delta_h$ | Disease mortality | 0.005 | day$^{-1}$ |
| $\Lambda_{v0}$ | Vector recruitment | 300 | vectors/day |
| $\mu_v$ | Vector mortality | 0.10 | day$^{-1}$ |
| $\sigma_v$ | Vector incubation | 0.15 | day$^{-1}$ |
| $\beta_{hv}$ | Vector–human transmission | 0.45 | day$^{-1}$ |
| $\beta_{vh}$ | Human–vector transmission | 0.35 | day$^{-1}$ |
| $a_T$ | Temperature sensitivity | 0.03 | $^{\circ}$C$^{-1}$ |
| $a_R$ | Rainfall sensitivity | 0.02 | rainfall-unit$^{-1}$ |
| $a_H$ | Humidity sensitivity | 0.015 | humidity-unit$^{-1}$ |

The initial conditions adopted for the simulations are

$$S_h(0) = 10{,}000, \quad E_h(0) = 50, \quad I_h(0) = 20, \quad R_h(0) = 0, \tag{48}$$

and

$$S_v(0) = 5{,}000, \quad E_v(0) = 100, \quad I_v(0) = 50. \tag{49}$$

These initial conditions represent the introduction of infection into a largely susceptible human population with an initially infected vector population.

It is important to note that the present simulations are scenario-based rather than empirically calibrated to observed climatic and epidemiological time-series data from the Niger–Delta region. The parameter values were obtained from relevant epidemiological literature and adjusted to provide representative baseline conditions for the study region. Thus, the numerical results are intended primarily to examine the qualitative and relative effects of climate variability on disease transmission rather than to provide direct outbreak forecasts. Empirical calibration and validation using long-term meteorological and epidemiological data from the Niger–Delta remain important areas for future research.

### *4.2. Case I: Baseline Climate Conditions*

The first simulation represents average climate conditions that do correspond with long-term meteorological records in the Niger Delta area. The climate variables stay at their base reference values and the whole setup is kept steady, no extra deviations in the background. In other words these variables are maintained at their different reference values and they remain fixed from there,

$$T = T_0, \qquad R = R_0, \qquad H = H_0. \tag{50}$$

With these conditions in place, the model shows a gradual rise in exposed people and infectious cases during the very early phase of transmission. After that, the number of infectious individuals reaches its peak first, and then it decreases as it moves toward an endemic steady state. The vector abundance stays approximately constant because the intake of new vectors and their removal, via mortality, keeps everything in balance.

The findings suggest that disease transmission continues whenever the basic reproduction number is above one, which points to the endemic nature of many vector-borne illnesses in the area.

### *4.3. Case II: Increased Temperature Conditions*

To look into possible impacts of climate warming, temperature was increased by 15% above its baseline value while rainfall and humidity stayed at their reference levels.

The simulations show a marked rise in transmission intensity, and also vector recruitment. When temperatures increase, the vectors mature faster and biting frequency increases; the pathogen incubation period gets shorter. As a result, infectious human cases increase more rapidly and reach higher peak levels than under the baseline scenario, indicating a compounded effect of the climatic conditions.

Overall, the findings point toward the fact that increasing temperature substantially increases disease transmission, and helps drive greater disease prevalence.

### *4.4. Case III: Increased Rainfall and Flooding Conditions*

Seasonal flooding keeps showing up as a recurring environmental problem in the Niger–Delta. To assess its effect, rainfall intensity was increased by $20\%$ above the baseline level, while the other climatic variables were kept at their reference values.

From the simulation results, the increased rainfall expands suitable vector breeding habitats, and it also improves vector recruitment. Because of that, vector abundance rises and disease transmission becomes more intense. In comparison with the baseline scenario, human infectious cases increase, they also stay elevated for a longer stretch, which then adds to the overall disease burden.

So these findings indicate that flooding plays an important role in keeping the disease around for longer periods in the Niger–Delta. Because of this, flood-control measures should be strengthened, drainage systems need better improvement, and environmental sanitation programmes must be treated as core actions, not just add-ons, for climate-adaptive disease control strategies.

### *4.5. Case IV: High Humidity Conditions*

In this scenario, relative humidity was increased by $10\%$ above its baseline value, while temperature and rainfall were maintained at their reference levels.

The results show a moderate lift in vector survival and disease prevalence. Even if the impacts are somewhat less obvious than those linked to temperature and rainfall, the longer vector lifespan matters, because it stretches the transmission season and increases the cumulative infection burden.

Overall, these findings suggest that humidity acts as an important secondary driver for disease persistence, especially in tropical environments.

### *4.6. Case V: Combined Climate Change Conditions*

To simulate future environmental conditions in a under a combined climate-change scenario, temperature, rainfall, and relative humidity were raised at the same time, based on the projected climate trends.

In this scenario, the epidemiological outcomes were the most severe. Vector recruitment increased markedly , transmission rates became stronger , and infectious populations climbed to much higher peak levels than the observed results when checking any one climate-change scenario on its own, independently.

Overall, the findings show that climatic variables do not act independently or additively like you might expect they do. Instead, they act together in a synergistic manner, which boosts the likelihood of sustained outbreaks and longer disease persistence, beyond what you would predict if you considered each variable separately.

### *4.7. Case VI: Climate-Adaptive Intervention Strategy*

A final simulation was done to check the effectiveness of climate-adaptive disease control measures. The intervention strategy in the model was represented by reductions in the climate-sensitive transmission and vector recruitment coefficients, thereby targeting both transmission and vector abundance simultaneously.

Overall, the results indicated strong drops in vector abundance, disease prevalence, and how long outbreaks last. Also, the basic reproduction number $R_0$ went down below the epidemic threshold when the intervention stayed in place over time, rather than just briefly.

Taken together, these outcomes indicate that climate-adaptive interventions can substantially reduce disease transmission and help maintain longer term disease control in the Niger–Delta region.

### *4.8. Comparative Analysis of Simulation Scenarios*

A comparison across all the scenarios really shows some notable shifts in how the disease behaves, like you can see it clearly. When temperature goes up, transmission efficiency gets the biggest boost. On the other hand, when rainfall increases, vector abundance climbs the most too. Humidity has a more moderate impact , mainly through its effect on vector survival not as dramatic as the first two factors.

under the combined climate-change scenario it produces the highest overall disease burden. Meanwhile the climate adaptive intervention scenario keeps landing as the lowest disease prevalence every time it's checked. The relative severity of the simulated climate scenarios, based on the corresponding values of the basic reproduction number, is summarized as

$$R_0^{\mathrm{CC}} > R_0^{\mathrm{RF}} > R_0^{\mathrm{HT}} > R_0^{\mathrm{HH}} > R_0^{\mathrm{BC}} > R_0^{\mathrm{CAI}}, \tag{51}$$

where

$$R_0^{\mathrm{CC}} = 0.3363, \quad R_0^{\mathrm{RF}} = 0.2602, \quad R_0^{\mathrm{HT}} = 0.1811,$$
$$R_0^{\mathrm{HH}} = 0.1753, \quad R_0^{\mathrm{BC}} = 0.1469, \quad R_0^{\mathrm{CAI}} = 0.0738.$$

Here, CC denotes Combined Climate Change, RF denotes High Rainfall, HT denotes High Temperature, HH denotes High Humidity, BC denotes Baseline Climate, and CAI denotes Climate-Adaptive Intervention. These values quantitatively confirm that the combined climate-change scenario has the highest transmission potential, whereas the climate-adaptive intervention produces the lowest.

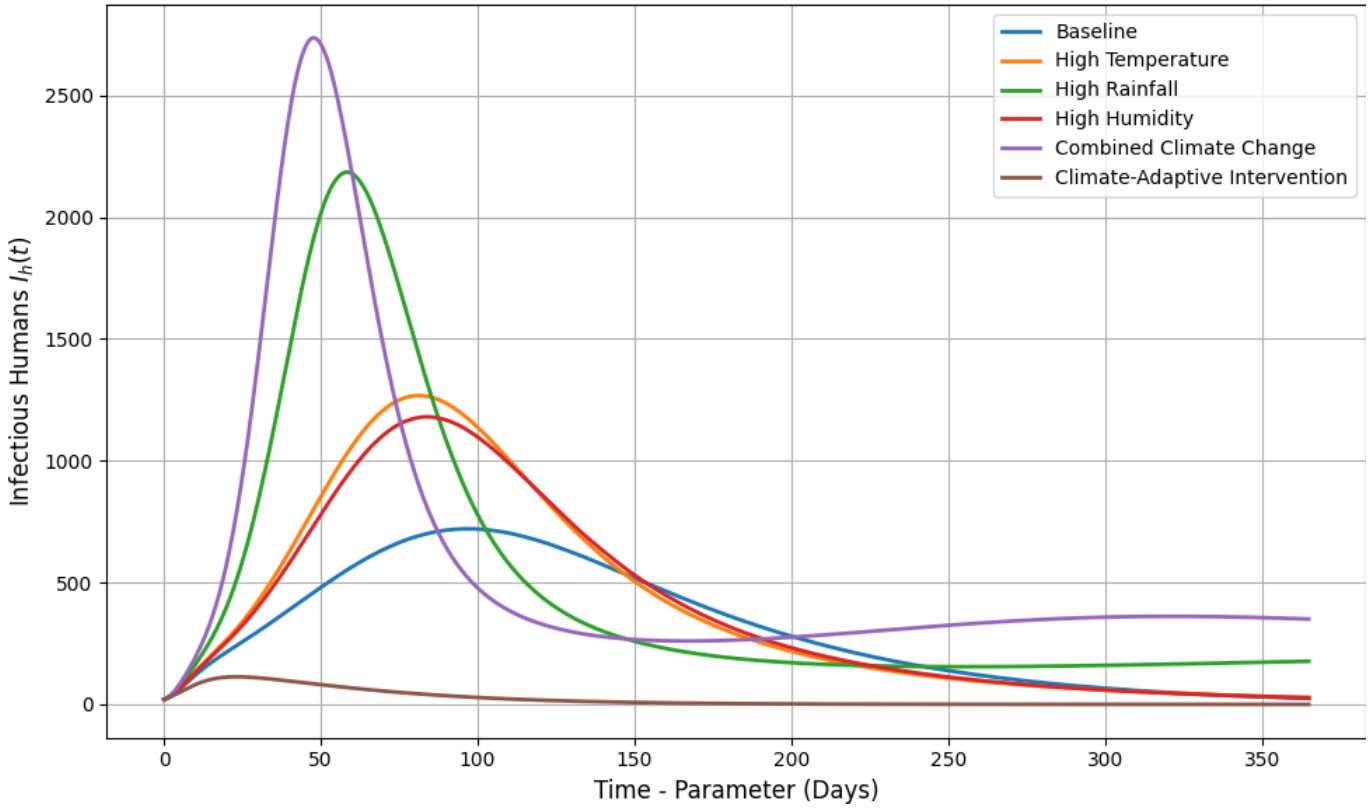


***Figure 2.*** *Human Infectious Population Under Different Climate Scenarios.*

Figure 2 shows the temporal dynamics of the infectious human population under the different climate scenarios. Increased temperature, rainfall, and humidity generally result in higher infection levels, with the combined climate-change scenario producing the greatest disease burden. In contrast, the climate-adaptive intervention substantially reduces the infectious population, highlighting the potential of integrated environmental and public health measures for disease control.

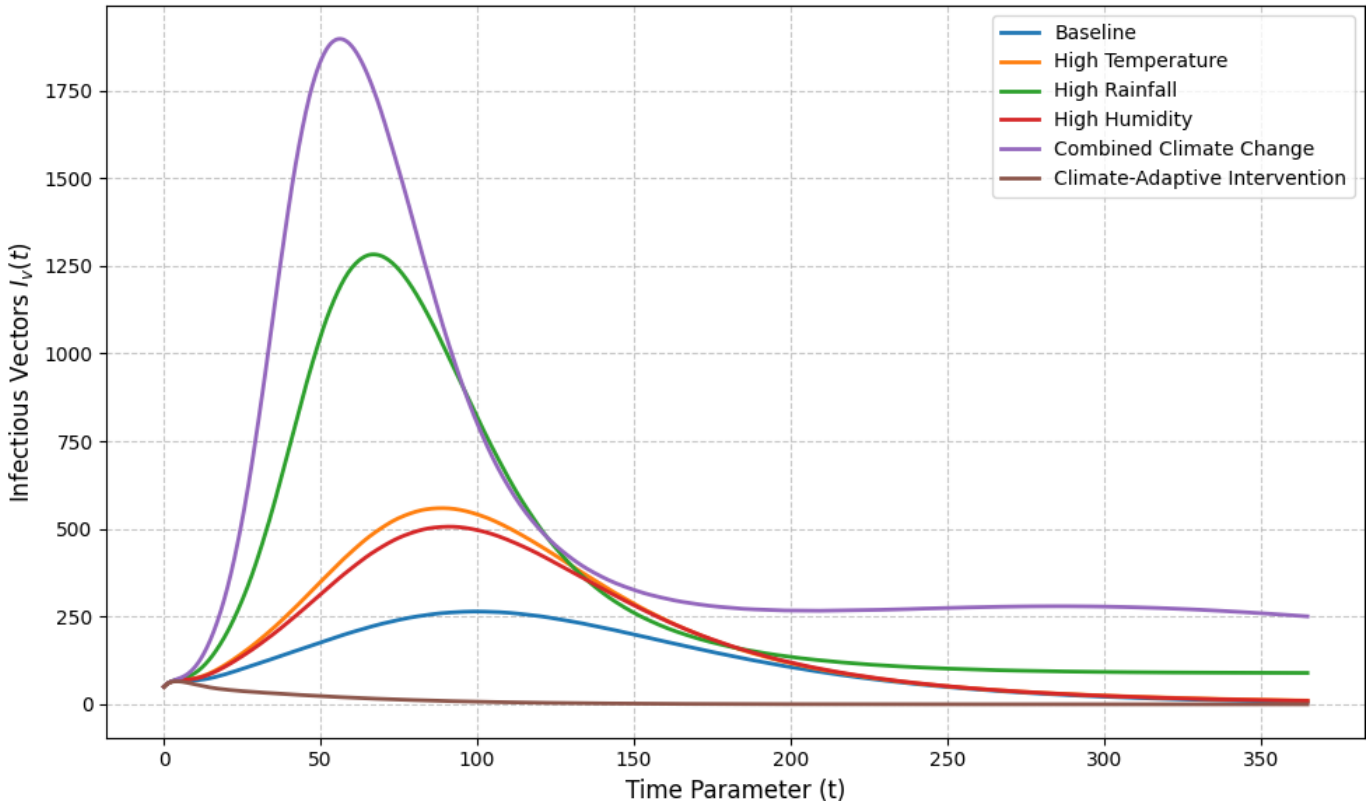


***Figure 3.*** *Infectious vector population dynamics under different climate settings.*

Figure 3 shows the dynamics of the infectious vector population under the different climate scenarios. Higher temperature, rainfall, and humidity generally increase vector infection levels, with the combined climate-change scenario producing the highest infectious vector population. In contrast, the climate-adaptive intervention markedly reduces vector infection and, consequently, transmission potential.

### *4.9. Remarks on the Numerical Findings*

The simulation results intensely support the theoretical findings as contained in Section 3. In particular, the dependence of the basic reproduction number $R_0$ on climate-sensitive transmission and recruitment parameters presents the observed increases in disease incidence under adverse environmental situations. The research findings show that climate change can considerably impact the epidemiology of vector-borne diseases in the Niger–Delta via its effects on vector ecology and environmental suitability. Increases in temperature, rainfall, and humidity enhance transmission potential and increase the likelihood of disease outbreaks.

From a policy point of view, the results highlight the importance of environmental management and climate adaptation approaches in disease control. Consequently, investments in drainage infrastructure, flood-control systems, environmental sanitation, vector habitat reduction, and climate-informed public health planning can significantly reduce disease burden and strengthen community resilience.

In all, the numerical simulations reveal that climate-sensitive epidemiological models are valuable tools for disease forecasting and for supporting evidence-based environmental health policy formulation in the Niger–Delta region.

#### *4.9.1. Comparative and Biological Interpretation of the Findings*

The findings are broadly consistent with previous climate-sensitive vector-borne disease modelling studies in Sub-Saharan Africa and Southeast Asia, where climatic variability has been associated with changes in vector abundance and disease transmission. However, the Niger–Delta presents a distinct environmental context, characterized by recurrent flooding, high humidity, extensive wetlands, and other environmental disturbances that may influence vector ecology and transmission dynamics.

Biologically, temperature can affect vector development, survival, biting activity, and pathogen development within vectors. Rainfall influences the availability of breeding habitats, while relative humidity affects vector survival and activity. The combined effects of these climatic factors therefore help explain the differences observed across the simulated climate scenarios.

#### *4.9.2. Model Limitations and Policy Implications*

The interpretation of the results should consider the assumptions of homogeneous host–vector mixing and the generalized representation of vector-borne disease. These assumptions do not account for spatial heterogeneity, population movement, behavioural differences, or pathogen-

specific biological characteristics. Consequently, the model is more appropriate for assessing general climate–transmission relationships and comparative scenario effects than for making pathogen-specific outbreak predictions. Future studies incorporating spatial heterogeneity, pathogen-specific characteristics, and empirical climate and epidemiological data would provide stronger support for localized disease surveillance, intervention planning, and public health policy.

# 5. Concluding Remarks

This present research developed a climate-sensitive mathematical model for exploring the transmission dynamics of vector-borne diseases in the Niger–Delta region of Nigeria. By incorporating these key climatic variables, viz, relative humidity, temperature, and rainfall, into a host–vector epidemiological framework, the model presents a quantitative hub for a clearer view of how environmental changes influence vector abundance and disease transmission. This is particularly important for regions that are highly vulnerable to the impacts of climate change. The basic properties of the model: existence and uniqueness of solutions, positivity, boundedness, and the characterization of a biologically feasible region were established via theoretical analysis. The disease-free equilibrium (DFE), $E_0$ and the endemic equilibrium (EE), $E^*$ were obtained and analyzed. In addition, the basic reproduction number $R_0$ was obtained as the threshold parameter governing disease persistence. It is noteworthy that, the stability analysis pointed out that the disease-free equilibrium of the system is locally and globally asymptotically stable whenever $R_0 < 1$, implying eventual disease elimination. From another perspective, a stable endemic equilibrium $E^*$ exists whenever $R_0 > 1$, reflecting sustained disease transmission within the population. Thus, these findings give a detailed mathematical framework for understanding the influence of climate variability on vector-borne disease dynamics and their long-term epidemiological effects and behaviour. Then, the numerical simulations showed that when temperature , rainfall, and humidity increase, vector recruitment, survival, and transmission potential all rise as well. After that, disease prevalence increases too, and the outbreaks tend to last longer. In the Niger-Delta region, when the combined climate-change scenario was applied, it produced the largest disease burden, which suggests that multiple climatic drivers are acting together in a more synergistic and amplified manner. This implies that public health risks could increase substantially. The simulations also showed that climate-adaptive interventions, such as environmental sanitation, stronger drainage systems, flood-control programmes, integrated vector management, and surveillance that follows climate patterns, can substantially reduce disease prevalence and reduce the basic reproduction number under the epidemic threshold. In general, these findings suggest that programmes for disease control should integrate environmental stewardship, climate adaptation with public health actions instead of treating them as separate parameters. From a practical perspective, the modelling framework we proposed works as a useful decision-support tool for policymakers, public health practitioners, and environmental managers. It can help with disease-risk forecasting, intervention appraisal, and more evidence-based allocation of resources in climate-sensitive areas. Despite its contributions, the study has some limitations. The model assumes homogeneous mixing between human and vector populations, and it does not explicitly account for spatial heterogeneity, population mobility, or even stochastic environmental fluctuations in a direct way. Also, the framework looks at vector- borne disease transmission in a generalized form, and it does not distinguish among specific pathogens, although they differ substantially in their biological characteristics. A further limitation is that the model assumes constant climate sensitivity coefficients for temperature, rainfall, and relative humidity. In reality, vector and pathogen responses to climatic conditions may be nonlinear and may exhibit threshold effects. Future studies should therefore consider nonlinear or threshold-dependent climate–response functions to better capture the biological responses of vectors and pathogens under varying environmental conditions. Future research may extend the model by incorporating spatial diffusion, stochastic effects, and heterogeneous population structures to better capture real-world disease dynamics. The integration of Geographic Information Systems (GIS), remote sensing technologies, and machine learning techniques could further enhance predictive accuracy and spatial forecasting capabilities. In addition, calibrating and validating the model using long-term epidemiological and meteorological data from the Niger –Delta region would improve its applicability for disease surveillance, outbreak prediction, and public health decision-making. Also, later work could inspect the economic repercussions that appear after climate- sensitive outbreaks, and compare the cost- effectiveness of various intervention options. In conclusion, this study suggests that climate change is a major driver behind the spread of vector- borne diseases across the Niger Delta region, and that disease control requires an integrated approach, mixing habitat management, climate adaptation , and public health actions, all together in a coherent way. The climate- sensitive modelling framework developed here provides a solid analytic instrument for tracking disease dynamics while environmental conditions keep changing, and it should give useful insights for sustainable environmental health policies and climate- resilient disease control strategies.

# ORCID

0009-0001-2341-1668 (Suit Patrick Oghenerhoro)
0009-0001-6230-5294 (Henry Etaroghene Egbogho)

## Abbreviations

| | |
|---|---|
| SEIR | Susceptible–Exposed–Infectious–Recovered |
| DE | Differential Equation |
| DFE | Disease-Free Equilibrium |
| EE | Endemic Equilibrium |
| RK4 | Fourth-Order Runge–Kutta Method |
| GIS | Geographic Information System |
| WHO | World Health Organization |

## Acknowledgments

The authors show deep appreciation to their respective institutions for a conducive research environment. They also wish to thank the editors and the anonymous reviewers for their constructive feedback. This study was funded by the Tertiary Education Trust Fund (TETFund), Nigeria, through the 2022&2024 Institution-Based Research (IBR) Intervention for Project SN 28-DOU-IBR, as communicated in TETFund Reference No.: TETF/DR&D/CE/UNI/ASABA/IBR/2022&2024/VOL.I.

## Author Contributions

**Suit Patrick Oghenerhoro:** Conceptualization, Investigation, Writing – original draft

**Henry Etaroghene Egbogho:** Data curation, Formal Analysis, Methodology, Writing – review & editing

## Conflicts of Interest

The authors declare no conflicts of interest.

## References

[1] B. Chala and F. Hamde, "Emerging and re-emerging vector-borne infectious diseases and the challenges for control: A review," *Frontiers in Public Health*, vol. 9, p. 715759, 2021.

[2] J. Ma, Y. Guo, J. Gao, H. Tang, K. Xu, Q. Liu, and L. Xu, "Climate change drives the transmission and spread of vector-borne diseases: An ecological perspective," *Biology*, vol. 11, no. 11, p. 1628, 2022.

[3] F. M. Chikezie, K. N. Opara, and P. M. E. Ubulom, "Impacts of changing climate on arthropod vectors and diseases transmission," *Nigerian Journal of Entomology*, vol. 40, pp. 179–192, 2024.

[4] N. Yadav and R. K. Upadhyay, "Global effect of climate change on seasonal cycles, vector population and rising challenges of communicable diseases: A review," *Journal of Atmospheric Science Research*, vol. 6, no. 1, 2023.

[5] J. M. Caldwell, A. D. LaBeaud, E. F. Lambin, A. M. Stewart-Ibarra, B. A. Ndenga, F. M. Mutuku, *et al.*, "Climate predicts geographic and temporal variation in mosquito-borne disease dynamics on two continents," *Nature Communications*, vol. 12, no. 1, p. 1233, 2021.

[6] G. Pavia, F. Branda, A. Ciccozzi, A. Romano, C. Locci, I. Azzena, *et al.*, "The issue of climate change and the spread of tropical diseases in Europe and Italy: Vector biology, disease transmission, genome-based monitoring and public health implications," *Infectious Diseases*, vol. 57, no. 2, pp. 121–136, 2025.

[7] S. E. Crawford, M. Brinkmann, J. D. Ouellet, F. Lehmkuhl, K. Reicherter, J. Schwarzbauer, *et al.*, "Remobilization of pollutants during extreme flood events poses severe risks to human and environmental health," *Journal of Hazardous Materials*, vol. 421, p. 126691, 2022.

[8] O. A. Dzyurdzya, V. V. Burlakov, G. V. Fedotova, E. V. Skubriy, and L. N. Orlova, "Climate change as a global threat to the world economy," in *Industry 4.0: Exploring the Consequences of Climate Change*, Cham: Springer International Publishing, pp. 13–21, 2021.

[9] C. O. Adio, C. D. Bando, A. Odawn, D. I. Dahutu, and S. C. Erhabor, "Climate change impact on microbial diseases in Nigeria: A review of emerging patterns and public health implications," *SSR Journal of Multidisciplinary (SSRJM)*, vol. 2, no. 4, pp. 17–33, 2025.

[10] S. O. Edeki, I. Adinya, M. E. Adeosun, and I. D. Ezekiel, "Mathematical analysis of the global COVID-19 spread in Nigeria and Spain based on SEIRD model," *Communications in Mathematical Biology and Neuroscience*, Article ID 84, 2020.

[11] L. C. Vieira, R. S. Costa, and D. Valério, "An overview of mathematical modelling in cancer research: Fractional calculus as modelling tool," *Fractal and Fractional*, vol. 7, no. 8, p. 595, 2023.

[12] S. Kumar, A. Srivastava, and R. Maity, "Modeling climate change impacts on vector-borne disease using machine learning models: Case study of visceral leishmaniasis (Kala-azar) from Indian state of Bihar," *Expert Systems with Applications*, vol. 237, p. 121490, 2024.

[13] M. Lecka, M. Omyła, E. Pietryszak, and M. Paruzel, "Impact of climate change on the spread of infectious diseases–review," *Journal of Education, Health and Sport*, vol. 82, pp. 60532–60532, 2025.

[14] J. C. Semenza, J. Rocklöv, and K. L. Ebi, "Climate change and cascading risks from infectious disease," *Infectious Diseases and Therapy*, vol. 11, no. 4, pp. 1371–1390, 2022.

[15] E. W. Ansah, M. Amoadu, P. Obeng, and J. O. Sarfo, "Health systems response to climate change adaptation: A scoping review of global evidence," *BMC Public Health*, vol. 24, no. 1, p. 2015, 2024.

[16] P. N. Schwerdtle, T. A. Ngo, F. Hasch, T. V. Phan, C. Quitmann, and C. A. Montenegro-Quinonez, "Climate change resilient health facilities: A scoping review of case studies in low and middle-income countries," *Environmental Research Letters*, vol. 19, no. 7, p. 074041, 2024.

[17] R. E. Baker, A. S. Mahmud, I. F. Miller, M. Rajeev, F. Rasambainarivo, B. L. Rice, *et al.*, "Infectious disease in an era of global change," *Nature Reviews Microbiology*, vol. 20, no. 4, pp. 193–205, 2022.

[18] Y. Wei, Z. Tian, M. Wang, Y. Zhao, and J. Wu, "Climate change impacts on human health: A systematic review of the literature," *Journal of Public Health*, vol. 44, no. 3, pp. 493–505, 2022.

[19] M. U. Kraemer, O. G. Pybus, C. Fraser, S. Cauchemez, A. Rambaut, and B. J. Cowling, "Monitoring key epidemiological parameters of SARS-CoV-2 transmission," *Nature Medicine*, vol. 27, no. 11, pp. 1854–1855, 2021.

[20] N. Shakiba, C. J. Edholm, B. O. Emerenini, A. L. Murillo, A. Peace, O. Saucedo, *et al.*, "Effects of environmental variability on superspreading transmission events in stochastic epidemic models," *Infectious Disease Modelling*, vol. 6, pp. 560–583, 2021.

[21] A. Almutairi, H. El-Metwally, M. A. Sohaly, and I. M. Elbaz, "Lyapunov stability analysis for nonlinear delay systems under random effects and stochastic perturbations with applications in finance and ecology," *Advances in Difference Equations*, vol. 2021, no. 1, p. 186, 2021.

[22] S. O. Edeki and V. E. Azu-Nwosu, "Deposit insurance modeling based on standard power option payoff using Picard–Lindelöf iteration," *Annals of Financial Economics*, vol. 19, no. 3, p. 2450013, 2024.

[23] R. Almeida, N. Martins, and C. J. Silva, "Global stability condition for the disease-free equilibrium point of fractional epidemiological models," *Axioms*, vol. 10, no. 4, p. 238, 2021.

[24] R. Nawaz, S. Kainat, N. M. A. B. N. Long, K. Shah, and T. Abdeljawad, "Fractal–fractional order mathematical modelling of co–infection dynamics of tuberculosis and diabetes mellitus with vaccination," *Journal of Applied Mathematics and Computing*, vol. 72, no. 2, p. 60, 2026.

[25] E. Acar, G. Bayrak, Y. Jung, I. Lee, P. Ramu, and S. S. Ravichandran, "Modeling, analysis, and optimization under uncertainties: A review," *Structural and Multidisciplinary Optimization*, vol. 64, no. 5, pp. 2909–2945, 2021.

[26] R. Nawaz, N. N. Long, and S. Shohaimi, "Caputo fractional differential equations for low-risk individuals of the tuberculosis transmission disease," *Malaysian Journal of Mathematical Sciences*, vol. 18, no. 4, pp. 919–947, 2024.